Comparison of DEM generation from SPOT stereo and ERS interferometric SAR data[1]

L. Renouard, F. Perlant, P. Nonin

ISTAR – route des Lucioles – Sophia Antipolis
06560 Valbonne – France
e-mail: Laurent.Renouard@istar.fr

ABSTRACT

In this paper, we compare Digital Elevation Models (DEMs) computed from SPOT image stereo pairs with DEMs obtained from ERS SAR interferometric pairs. After reviewing satellite DEM data sources, the correlation and interpolation algorithms used for producing SPOT DEMs are presented. We determine the error in SPOT DEMs by analysing the influence of slope on the altimetric error σZ, and the theoretical model is evaluated on a region of the Alps. We present the ERS interferometric DEM computation method: construction of the interferogram, phase unwrapping, and geometric modelling of the interferometric pair. We compare SPOT DEMs (7 m precision) with ERS DEMs on a 100 km x 100 km section of Utah. From this comparison, ERS DEM precision can be evaluated as 20 m, taken between 1/3 and 1/4 of the ambiguity height, and we establish an empirical relation for interferometric DEMs between the error and the slope.

1. INTRODUCTION DEMS FROM SATELLITE IMAGES

The production of DEMs from satellite images is a constantly changing field. In the last 10 years, both the sources of data as well as production techniques have greatly multiplied. SPOT stereoscopic pairs, available since 1986, are processed using automatic correlation, and a number of companies specialized in this technique, including ISTAR, offer commercial products. More recently, in 1992, SAR interferometric DEM was developed, where the DEM is obtained from interferometric pairs of ERS 1 images by unwrapping the interferogram phases. Other techniques for producing DEMs are being studied: stereoscopy and clinometry using SAR data, and shape from shading techniques using optical data. New sources of data now available include space photographs MK4 and TK350 from Russian satellites, and stereoscopic images from the MOMS 2 German sensor. Nowadays, using SPOT for producing DEMs is the standard method (where images are available), whereas producing DEMs by using ERS interferometry could be the method of the future.

Keywords: DEM, Interferometry, SPOT, ERS, Stereoscopy

1. This work was supported in part by ESA under contract n° 134005.

2. SPOT OPTICAL STEREO

2.1 Producing SPOT optical stereo DEMs

Stereoscopy is traditionally used to measure the variations of parallax between two images of the same scene, taken from different angles. The absolute positions of the ground points in a cartographic projection are computed from this parallax measurement in a two-step process. The first step computes the parallax map, also called the disparity map, and the second uses geometric modelling to project the disparity map into a system of cartographic coordinates to obtain the DEM.

2.2 Disparity map computation Correlation along lines

We describe the techniques used at ISTAR. First, the left image is resampled in the geometry of the right image eliminating the residual parallax in y (L. Renouard, 1992) in order to reduce the matching problem to a one-dimensional problem. This can also be done by resampling both images in epipolar geometry.

Different types of correlation techniques exist, the one we describe is based on a dynamic programming algorith.

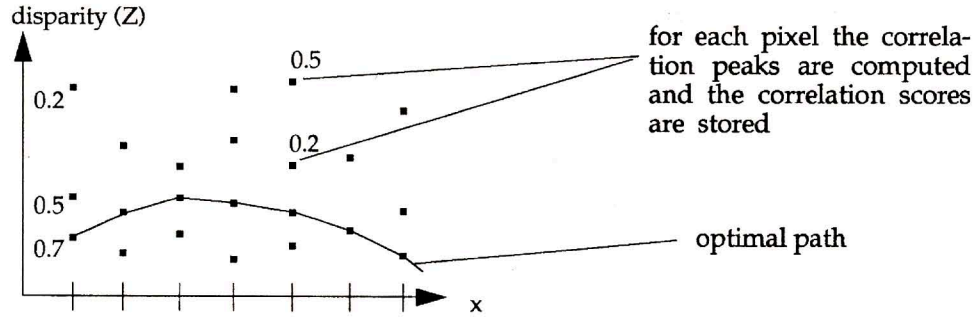

Figure 1 - Correlation techniques based on a dynamic programming algorithm.

The correlation peaks are computed for each pixel (figure 1), and the correlation scores are stored.

We then find the path which maximizes the sum of the correlation scores, *C(path)*, under ordering constraints (we eliminate paths with local derivative less than -1).

The disparity map thus computed is then interpolated by using a relaxation technique. We minimize a sum of three energy terms: one term for the data, a second term assuming that the terrain behaves as a thin plate giving good rigidity to the solution, and a third term using a membrane model to give continuity to the solution. The convergence of the solution is obtained by a multiresolution Gauss-Seidel algorithm.

$$E = \beta\Sigma(S - S_{i,j})^2 + \alpha \int \left(\frac{\partial^2 S^2}{\partial x^2} + 2\frac{\partial^2 S^2}{\partial x \partial y} + \frac{\partial^2 S^2}{\partial y^2} \right) dxdy$$

$$+ (1-\alpha) \int \left(\frac{\partial S^2}{\partial x} + \frac{\partial S^2}{\partial y} \right) dxdy$$

2.3 SPOT stereo error model

Optical stereo error models were proposed by (I. Dowman, 1990), (L. Renouard, 1991). Our most recent model for SPOT (eq. 1) gives the average quadratic deviation in height σZ with respect to certain parameters:

- r, the pixel size at the nadir, (r = 10 m for panchromatic SPOT);
- σc, the precision of the correlation process, (σc = 0.5 with our correlator and SPOT images);
- b/h, the base to height ratio of the stereo system;
- α_l, the angle of the viewpoint of the left image;
- α_t, the angle of the viewpoint of the right image;
- s_x, the slope of the terrain in the parallax direction.

$$\sigma Z = \frac{r \cdot \sigma c}{b/h} \times max\left(\frac{1}{cos\alpha_r \, cos(\alpha_r - s_x)}, \frac{1}{cos\alpha_l \, cos(\alpha_l + s_x)} \right)$$

Eq. 1 SPOT stereos error model

This model is suitable for slopes less than 30 degrees.

The DEMs next page show an example in the French Alps, the comparison of an IGN[1] reference DEM (figure 2) and an optical SPOT DEM (figure 3).

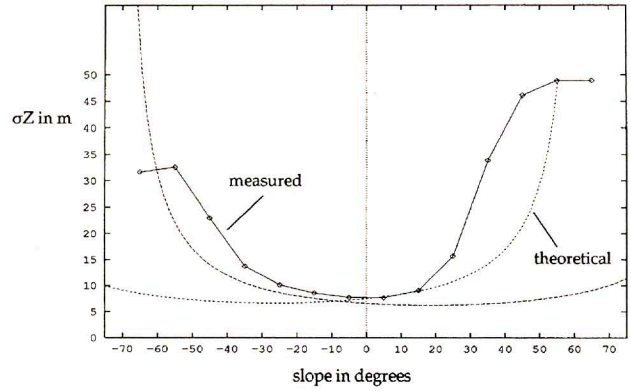

The figure above shows the result in the French Alps comparing the theoretical model and the errors (figure 4) measured with respect to the slope (figure 5).

For this comparison, the parameter values are: b/h = 0.84, α_l = 18.5°, α_r = 26.9°, the reference is the IGNDEM (figure 2) with precision $\sigma Z_{reference}$ = 5 m. The measured precision of the SPOT DEM (figure 3) is σZ = 10.5 m. The height variation in the zone is Z = 2,000 m.

For slopes greater than 30 degrees in both directions (parallax and perpendicular to the parallax) other phenomena have to be taken into account: interpolation technique, shadows, quality of the terrain selected to verify the model.

1. Institut Géographique National – France.

Figure 2 - IGN DEM (Reference) – σZ = 5 m.

Figure 3 - SPOT DEM – σZ = 10.5 m.

Figure 4 - Errors in Z.

Figure 5 - Slopes in x.

3. ERS INTERFEROMETRIC DEM

3.1 Producing interferometric DEMs the interferogram

Radar interferometry experiments have already been conducted for a number of years, but it is only recently that the interferometry technique from satellite radar has been demonstrated (H. Zebker, 1986).

The ERS interferometric DEM is produced in several steps (F. Perlant, 1994). First, a raw pair of ERS 1 type images is acquired with an inter-track that fulfils the interferometric conditions. Our interferograms are produced by the CNES[1]. Correlation makes it possible to determine the exact translation to apply to resample the first image in the geometry of the second image.

1. CNES – French Space Agency.

Let us keep in mind that the geometric variations are sub-pixel, and that matching must preserve the signals as much as possible in order to guarantee the coherency between the two overlaid images (D. Massonnet, 1991).

After this processing the complex value of the right-hand image is multiplied by the conjugate value of the left-hand image, and the argument of this scalar product gives the difference in phase for each pixel. This phase difference is corrected by a polynimial surface so that the complexity of the phase unwrapping stage is minimized.

3.2 Unwrapping the interferogram

The usual method of phase unwrapping consists in integrating the phase differences along an arbitrary path so that the final phase difference between two adjacent pixels is between $-\pi$ and π radians.

Noise and phase aliasing corresponding to high reliefs show up as integration errors which propagate. Various techniques using fringe lines (Q. Lin, 1991) or "ghost lines" (C. Prati, 1990) try to overcome these difficulties. Using simulated interferograms we have developed another approach based on interfringe regions (an interfringe region is a homogeneous region between two successive fringe lines).

The interferogram is unwrapped by image processing techniques. We apply successively elimination of the phase noise (or local filtering), segmentation into adjacent interfringe regions presenting good spatial coherency, and connection of the various regions between themselves. Constraints related to overlapping and shadow zones can be introduced before segmentation into regions in order not to take into account the phase noise in those regions.

Figure 6 shows the phase unwrapping for the portion of an interferogram over a region of Utah.

3.3 Geometric modelling

The geometry of the interferometric pair (figure 7) is modelled from auxiliary data (the two registered orbits of the interferometric pair are supplied with the interferogram), and from ground control points plotted on maps. There are two steps to modelling with ground control points ($N > 10$): first a low frequency registration step of the geometry of the master image (amplitude 20 m), then a high frequency registration step of the geometry of the slave image (amplitude on the order of 1 cm).

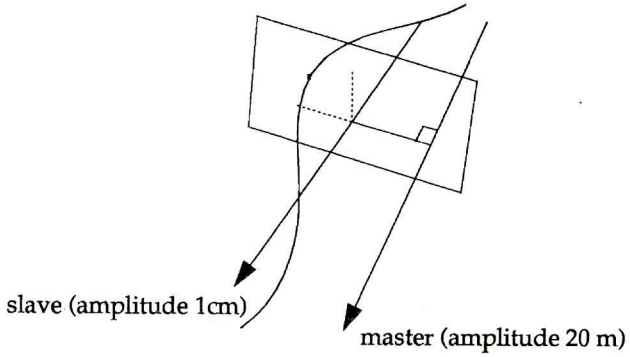

Figure 7 - Principle of geometric modelling of the interferometric pair.

The modelling allows transformation of any pixel from pixel coordinates x, y and absolute phase shift ϕ into a geocoded pixel (for example in a UTM projection) with its height value. In this process, layovers create holes in the geocoded altimetric data. After interpolation, the interferometric DEM is obtained.

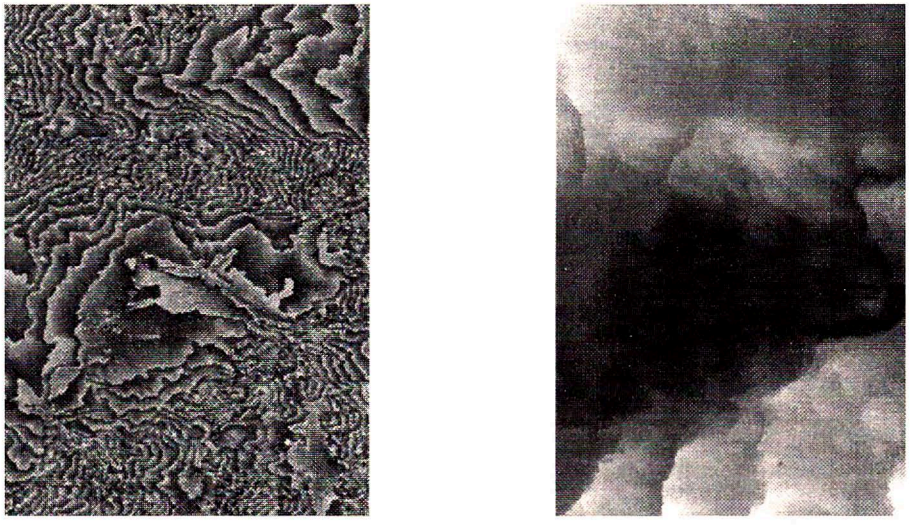

Figure 6 - Utah, interferogram (left), unwrapped phases (right).

3.4 Example of ERS 1 interferometric DEM

The figures below (figures 8-11) show a 100 km x 100 km example of ERS 1 interferometric data set over Utah. This interferometric pair was acquired on orbits 4380 of May 17 th 1992, and 4881 of June 21st 1992 with 35 days in between. It satisfies the interferometric conditions : the inter-track (distance between the two successive tracks of the satellite) varies from 162 m to 171 m during the acquisition of the scene. The ambiguity height (height variation corresponding to a fringe) varies at the four corners of the scene: 62 m at the NE corner, 43 m at the NW corner, 59 m at the SE corner, and 41 m at the SW corner.

3.5 Comparison of SPOT DEMs and ERS DEMs

In order to evaluate the precision of the ERS-1 DEM we compare it with a 7 m altimetric precision SPOT DEM (figure 12). The SPOT DEM was resampled at 40 m resolution and compared to the ERS-1 interferometric DEM in the same projection and also at 40 m resolution.

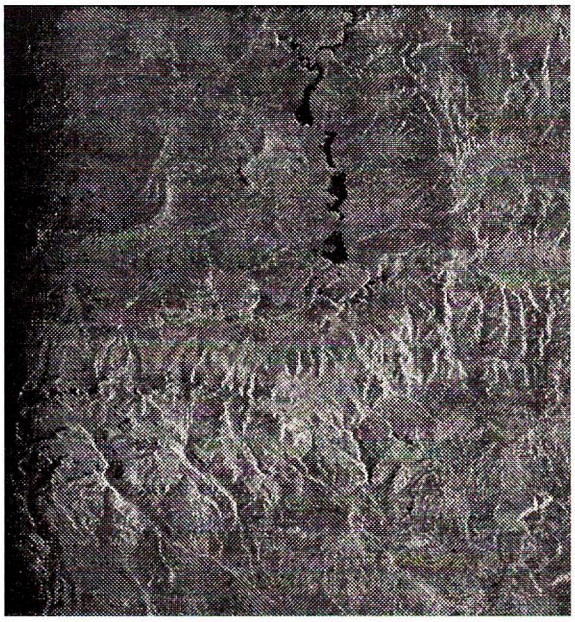

Figure 8 - Module image.

Figure 9 - Coherence image.

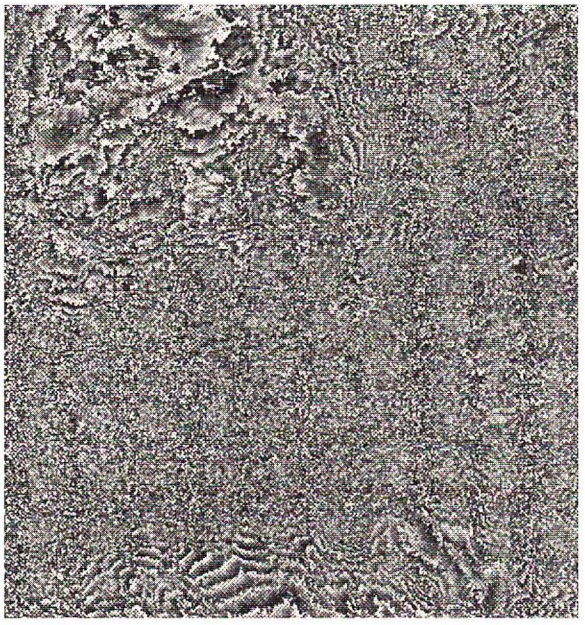

Figure 10 - Phase image.

Figure 11 - Unwrapped phase image.

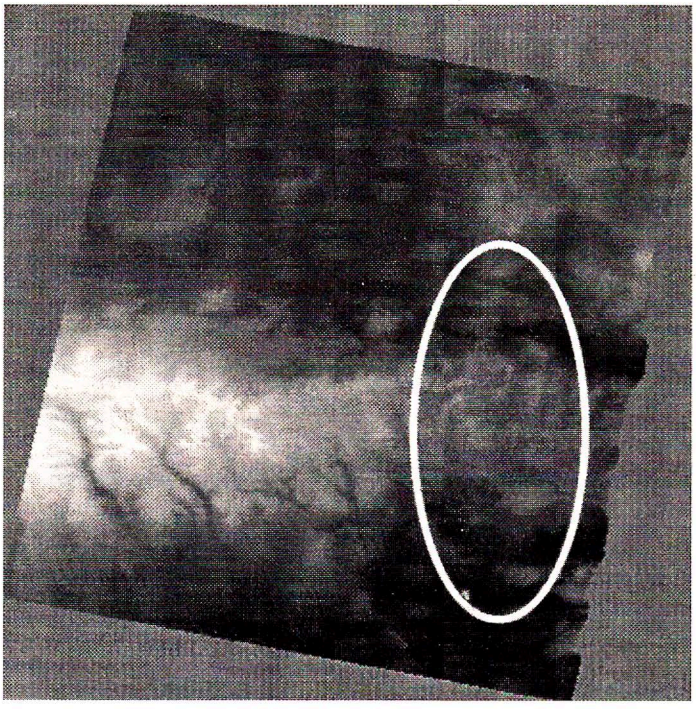

Outlined zone = overlapping zone

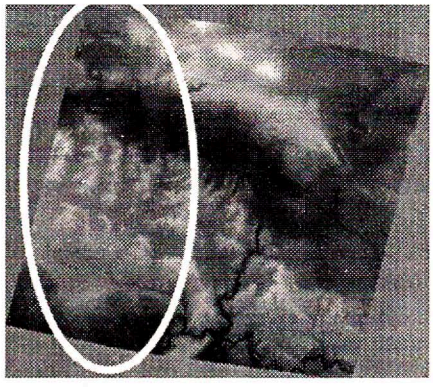

ERS DEM – 120 km x 120 km
σZ = 20.5 m

SPOT DEM 80 km x 70 km
σZ = 7 m

Figure 12 - Comparison of the ERS DEM (left) and the SPOT DEM (right).

The two DEMs overlap only partially so that we can compare them only on a region of 20 km x 60 km. In order to dissociate the phase unwrapping problems from the altimetric precision problems, we manually adjusted the unwrapped phases for this portion of the image. Thus the portion of the ERS-1 DEM results shows very few local errors.

The difference between both DEMs gives us an altimetric error of 20.5 m at 1 σ for this 20 km x 60 km zone. Considering the SPOT DEM error (7 m) we can regard this value as the statistical error of the ERS-1 DEM at 1 σ. This value, 20 m, corresponds to 1/3 of the ambiguity height which is 60 m in the East part of the interferometric DEM.

A more detailed analysis shows that the relative precision of the interferometric ERS DEM is locally better than 20 m at 1 σ. If we eliminate the low frequency component of the error, we obtain a relative precision of 10 m at 1 σ (i.e., 1/6 of the ambiguity height).

Moreover, certain details in the ERS DEM are not visible in the SPOT DEM, and vice-versa. In particular, all the steep slopes oriented towards the satellite (layover) had to be interpolated in the ERS-1 DEM. The altimetric information is missing for these zones.

3.6 Error model for the ERS interferometric DEM

On a nearby site we tried to carculate an error model with respect to the terrain slope. The first results are incomplete, but confirm that the ERS DEM error is very sensitive to the terrain slope in the direction perpendicular to the satellite trace.

The conditions of this test over a zone of Utah are: intertrack of 250 m, ambiguity height of 45 m, height variations in the 1,000 m zone, the reference is a SPOT DEM of 8 m precision at 1 σ.

The ERS DEM is raw (no interpolation) over the zones where the phase unwrapping was possible; it is interpolated for the overlapping and layover zones. The statistical precision at 1 σ of the ERS DEM is 12 m corresponding to 1/4 of the ambiguity height. The error depending on the terrain slope in the direction perpendicular to the satellite track varies as shown figure 13.

4. CONCLUSION

We compared the optical stereo-reconstruction and ERS-1 SAR interferometric techniques over 2 sites in Utah.

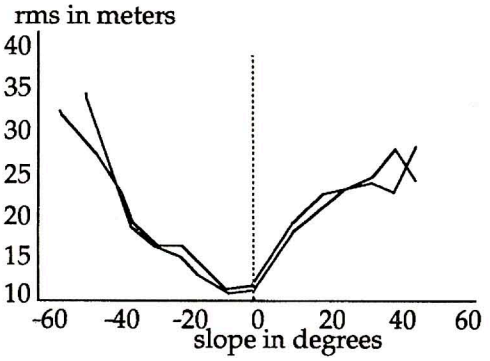

Figure 13 - Error as a function of slope for the ERS DEM.

Generating DEMs by SPOT stereo-reconstruction is a proven technique with which ISTAR has already produced over 1 million square kilometres. The image (correlation) and geometric processing aspects are now well-understood and we can model the altimetric error. However there are limitations for very steep slopes (> 30 degrees).

Generating DEMs by SAR interferometry is a recent technique. Early results demonstrate its potential but there are only few examples. The signal processing (generating the interferogram and phase unwrapping) and geometric processing aspects have not yet been completely mastered. In particular, the sensitivity of the geometric model when selecting ground control points, as well as the presence of phase differential phenomena, give altimetric precision inferior to those we would expect given the ambiguity height.

Nowadays the precision obtained for the ERS-1 DEM is on the order of 1/3 to 1/4 of the ambiguity height, whereas the noise level in the unwrapped phases holds promise for a precision on the order of 1/10 to 1/20 of the ambiguity height.

Therefore, measurement of the phase difference quality alone and its coherency is not enough to model the error on the resulting DEM. Side-looking geometry is also an important parameter to integrate into the altimetric error modelling. In addition the inter-track distance which characterizes the ambiguity height has its limits. For instance, increasing this distance can reduce the ambiguity height, and therefore increases the altimetric precision of the resulting DEM, but phase coherency, aliasing, and phase unwrapping problems limit the potential gain in precision. We have presented certain limitations, some of which will find a solution only by using complementary data: ground control points, a DEM to help phase unwrapping, and multiple interferometric pairs.

We can conclude that the stereo-reconstruction and SAR interferometry approaches are similar. The current automation levels are equivalent, and the processing operations are very much alike. These two techniques based on SPOT and ERS-1 present potential precision very close to the specific limitations of each method. SAR interferometry and optical stereo-reconstruction can therefore be considered as complementary.

5. REFERENCES

Dowman I., 1990, Heighting Accuracy of SPOT, IEEE trans. 1991.

Lin Qian, Vesecky John F. & Zebker Howard A., 1991, Topography estimation with interferometric synthetic aperture radar using fringe detection, IEEE Trans. Geoscience Remote Sensing, 1991.

Massonnet D. & Rabaute Th., 1991, Radar interferometry: Limits and Potentials, presentation at PIERS, Boston 1991, Submitted to IEEE.

Perlant F., 1992, Use of CNES Interferometric Product, PIERS 1994, Nordweg, July 1994.

Prati C., Rocca F., Guarnieri A.M. & Damonti E., 1991, Seismic migration for sar focusing: Interferometrical applications, IEEE Trans. Geoscience Remote Sensing, vol. 28, pp. 627-640, July 1990.

Renouard L., 1991, p. 93 à 115, Extraction automatique du relief à partir de couples stéréoscopiques d'images du satellite SPOT, Thèse de Doctorat. École Polytechnique 1991.

Renouard L., 1992, ISPRS, MNT à différentes résolutions par stéréo optique, ISPRS Com IV, Washington 1992 (Proceedings).

Zebker H.A. & Goldstein R.M., 1986, Topographic mapping from interferometric SAR observations, Journal of Geophysical Research, vol. 91, n° B5, October 1986.